Journal of Applied Electrochemistry **29**: 1291–1296, 1999.

Transient and turbulent mass transfer in rotating shallow electrochemical cells

F.-B. WENG, Z. CHENG, Y. KAMOTANI* and S. OSTRACH
*Department of Mechanical and Aerospace Engineering, Case Western Reserve University, Cleveland, Ohio 44106 (*author for correspondence, e-mail: yxk@po.cwru.edu)*

Received 19 November 1998; accepted in revised form 4 April 1999

Key words: local current density, mass transfer, onset of transient, rotating electrochemical cells, turbulent convection

Abstract

Turbulent mass transfer in a rotating shallow electrochemical cell was investigated experimentally. Six local miniprobes embedded in the cathode were used to measure the local mass transfer rate and to detect unsteady turbulent convection. The mass transfer rates were nondimensionalized and correlated. A critical parameter was obtained to describe the onset of transient and turbulent conditions in the rotating electrochemical cells. The transient and turbulent phenomena in the rotating system are more complex than natural convection in vertical enclosures because of gravity-gradient effects.

List of symbols

Ac	acceleration ratio ($\Omega^2 R\ g^{-1}$)
Ar	aspect ratio ($H\ R^{-1}$)
$\bar{C}, C$	dimensional and dimensionless Cu^{2+} ion molar concentrations (M, mol l^{-1})
$\bar{C}_b$	Cu^{2+} ion bulk molar concentration (M, mol l^{-1})
D	mass diffusion coefficient ($cm^2\ s^{-1}$)
Ek	Ekman number ($v\Omega^{-1}H^{-2}$)
g	gravitational acceleration ($g = 981\ cm\ s^{-2}$)
H	thickness of test cell (cm)
h	total mass transfer coefficient ($cm\ s^{-1}$)
$h(r)$	local mass transfer coefficient ($cm\ s^{-1}$)
i	current density ($mA\ cm^{-2}$)
R	radius of test cell (cm)
Ra	Rayleigh number in natural convection ($g\beta_T \Delta T L^3\ (v\alpha)^{-1}$)
Ra_R	centrifugal Rayleigh number ($\Omega^2 \beta \Delta C R^4\ (vD)^{-1}$)
Ro_S	solutal Rossby number ($\beta \Delta C$)
r	dimensionless radial coordinate
Sc	Schmidt number ($v\ D^{-1}$)
$Sh(r)$	local Sherwood number based on cell thickness ($h(r)H\ D^{-1}$)
$\overline{Sh}_R$	total Sherwood number based on cell radius ($hR\ D^{-1}$)

Greek symbols

β	volumetric expansion coefficient due to concentration change (M^{-1}, 1 mol^{-1})
v	kinematic viscosity ($cm^2\ s^{-1}$)
	Cu^{2+} ion molar concentration difference between two electrodes, $\Delta C = 2\bar{C}_b$ (M, mol l^{-1})
ρ	density ($g\ cm^{-3}$)
Ω	rotation speed (rpm, 0.1047 rad s^{-1})

1. Introduction

The present research was motivated by the discovery of a rotating nickel–zinc battery system. The development and commercialization of a Ni/Zn battery system has been hindered for decades mainly due to the limited cycle-life of the zinc electrode [1]. By rotating the battery, which consists of a stack of bipolar cylindrical cells, at a few hundred rpm., the battery performance and cycle-life can be improved dramatically [2]. The following effects have been noticed: (i) the dendrite growth is eliminated and the zinc electrode material redistribution is stabilized, prolonging battery life to 1000 cycles, (ii) the charging and discharging current density is increased five times over the current density of non-rotating Ni/Zn battery. The rotating Ni/Zn battery technology has commercial potential to replace the nickel–metal hydride battery for hybrid vehicle applications because of its high power density, low material costs and long cycle-life. The successful improvement of the battery has been attributed to the well-behaved solutal convection in the rotating battery. The mass transfer process in the rotating electrolyte solution is complex. With superimposed rotating motion in the charging cells, the solutal buoyancy induces a swirling secondary flow through the coupling among centrifugal, Coriolis and gravitational accelerations as well as variation of density in the electrolyte solution. In the meantime, the rotating electrochemical systems have

become increasingly important in conjunction with the human exploration and development of space. The present study could advance efficient design of life support systems and energy storage systems in microgravity environment.

We have investigated, experimentally and theoretically, laminar mass transfer in rotating electrochemical cells [3, 4]. Based on scaling analysis we found various important dimensionless parameters, classified the flow and solutal fields according to those parameters, and obtained expressions for the total mass transfer rate. We also computed the flow and solutal fields numerically and showed that the results agree with those from the scaling analysis and experimental data except when unsteady mass transfer was experimentally observed at high rotation rate and concentration difference. Moreover, some implications of our results to Zn/Ni battery applications were described. Strong centrifugal convection can enhance the limiting currents, so that the battery power density increases, the recharging time decreases, and the dendrite formation is minimized. The shape change of the zinc electrode could be prevented by increasing the mass transfer near the edge regions. The shape change phenomenon is that the active zinc materials move from the edge to the centre region after several hundred recharging cycles [1].

As the rotating systems scale up for large battery applications, the mass transfer could become transient and turbulent. The Coriolis and gravity-gradient effects of rotating cells become increasingly important. The purpose of the present work is to measure local mass transfer rates. With embedded miniature probes on the cathode of the test cell, the limiting current method with a cupric sulfate–sulfuric acid system is used to study the local mass transfer rates and transient behaviour in the rotating cell. The critical parameter to determine the transient or turbulent convection is investigated.

2. Experimental setup and procedure

A schematic of a rotating shallow electrochemical cell is shown in Figure 1. The rotating facility and the detail of test section are given in Figure 2. The experimental rotating facility was described earlier [4]. The test section consisted of two horizontal circular electrode copper discs, an electrolyte solution, a Viton gasket, one reference copper probe and six miniature probes, as well as two circular aluminium sheet covers. The diameters of two electrodes were both 30.5 cm, with an actual working area of 729.6 cm^2. The Viton gasket was 30.5 cm ID, 35.5 cm OD and 0.64 cm thick. The six miniature probes of diameter 0.63 cm were distributed on the cathode to measure the local mass transfer rate [5]. As shown in Figure 2, the locations of the six insulated miniature probes were 2.54 cm (p1), 5.08 cm (p2), 7.62 cm (p3), 10.2 cm (p4), 12.06 cm (p5) and 13.97 cm (p6) from the centre of the cathode. Another miniprobe made of copper tube was placed at the centre of the cathode for use as a reference potential probe and as an electrolyte filling tube. Air bubbles escape from the test cell through an orifice on the edge of the test section during the filling of the electrolyte solution. The solution was a cupric sulfate solution with 1.5 M sulfuric acid as supporting electrolyte ($CuSO_4$–1.5 M H_2SO_4). The advantages of this solution are slow roughness development, well-known electrochemical reaction and similar fluid properties to the zincate–alkaline solution. A HP-1B DC (6641A) power source supply, manufactured

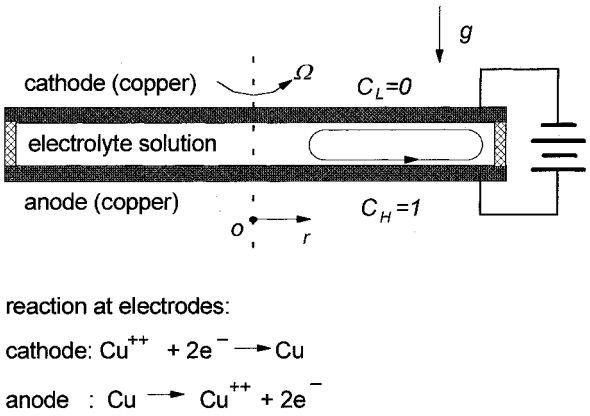

Fig. 1. Schematic diagram of the rotating shallow electrochemical cell. Electrolyte composition: $CuSO_4$–1.5 M H_2SO_4.

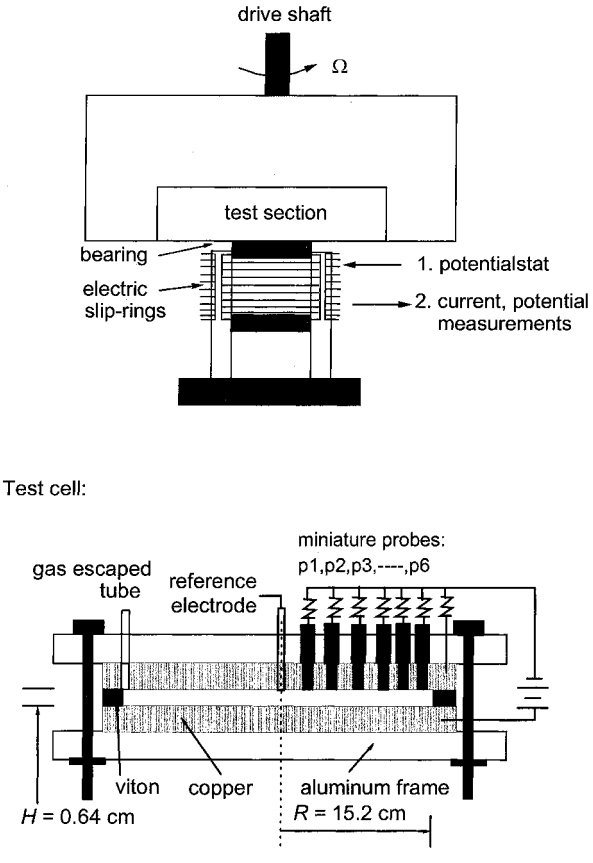

Fig. 2. Rotating facility and assembled test cell.

by Hewlett-Packard, provided complete flexibility in potential or current control for the electrochemical experiment. A high speed voltage measurement system, OMB-TempScan-110 and TempV/32 module (a product of Omega Co.), was used for the current and voltage measurements.

With the present experiment setup, the anode, where copper dissolves was at the bottom (Figure 1). Since the fluid is denser at the anode, the solution is gravitationally stable, meaning that no fluid motion occurs without rotation. However, with rotation, convection is set up by centrifugal buoyancy in such a way that the fluid moves radially outward along the bottom wall and radially inward along the top wall (Figure 1).

To minimize the error due to the initial surface roughness, the surface of the electrode was carefully polished. The polishing process began with emery paper 200, and progressed sequentially to 600. The working surface of the electrode was washed with tap water followed by distilled water. Technical grade methanol was applied in the final step to dry the surface and to increase the wetting action of the electrolyte solution.

The mass transfer rate was determined by measurement of limiting currents. The limiting current method for measuring the mass transfer rate in electrochemical systems has been described by Selman and Tobias [6]. To determine the limiting current the potential difference between the working electrode and reference probe was increased stepwise, starting from zero, and the current monitored. At each potential setting, the current quickly approached a quasi-steady state (2–3 min). The experiment was terminated immediately following establishment of the limiting current plateau to avoid excessive hydrogen evolution.

The experimental conditions were: radius $R = 15.2$ cm, height $H = 0.64$ cm, mass diffusion coefficient $D = 4.86 \times 10^{-6}$ cm^2 s^{-1} at 25 °C, kinematic viscosity $v = 1.16 \times 10^{-2}$ cm^2 s^{-1} at 25 °C, volumetric expansion coefficient $\beta = 0.118$ M^{-1}, concentration difference between the electrodes $\Delta C = 0.02$ M ~ 0.16 M and rotation speed of the test section $\Omega =$ 100 rpm $\sim$ 400 rpm (10.5 $\sim$ 41.9 rad s^{-1}). The above physical properties are obtained from the work of Wilke et al. [7].

3. Important dimensionless parameters

The important dimensionless parameters in the present experiments are (Weng et al. [4]): Ek, Ro_S, Sc, Ar, and Ac. The parameter Ek represents the ratio of velocity boundary layer (Ekman layer) thickness along the electrode surface to the test cell height (H). In the present experiment, Ek is always less than unity so that the radial motion of fluid along the electrode is confined to the relatively thin velocity boundary layer. The parameter Ro_S represents the ratio of characteristic fluid velocity to rotation velocity (ΩR). In the solutal convection driven by centrifugal buoyancy, the characteristic velocity can be set to $\Omega R\beta\Delta C$, then Ro_S is equal to $\beta\Delta C$. The parameter Sc is equal to the ratio of fluid kinematic viscosity to mass diffusion coefficient. Sc is much larger than unity for the present test fluid. Weng et al. [4] showed that the combined parameter $Sc\,Ro_S$ plays an important role in the present problem. The parameter $Sc\,Ro_S$ represents the ratio of velocity boundary layer thickness to solutal layer thickness and determines the convection regimes. In addition, Ek and $Sc\,Ro_S$ are sometimes combined to form Ra_R, which corresponds to Rayleigh number in natural convection. Ar is much less than unity for the present test section to simulate a shallow battery cell. Ac is the ratio of centrifugal acceleration to gravitational acceleration. The local and total mass transfer rates are nondimensionalized as the local and total Sherwood numbers, respectively.

The ranges of dimensionless parameters corresponding to the above experimental conditions are: $Ek = 6.9\times10^{-4}$–2.8×10^{-3}, $Ro_S = 2.4\times10^{-3}$–1.9×10^{-1}, $Ac =$ 1.70–27.3, $Ar = 0.042$, $Sc = 2380$, $Ra_R = 2.3\times 10^{11}$–3.0×10^{13} and $Sc\,Ro_S = 5.3$–42.7. Since $Sc\,Ro_S$ is larger than unity, the flow field is dominated by centrifugal convection in the radial direction (Weng et al. [4]). The effect of gravity can be neglected in the above range of Ac. The estimated errors for the dimensionless parameters are: $Sc\,Ro_S$ within 10%, Ek 5%, Ac 2%, Ra_R 11% and $\overline{Sh}_R$ within $\sim$11%.

4. Results and discussion

Figure 3 shows the local current density polarization curves for the six miniature probes under the conditions of 0.02 M bulk concentration and 200 rpm rotating speed. At each location the current density increases with increasing overpotential up to about 300 mV, beyond which the slope of current–overpotential curve decreases noticeably. It is known generally that the limiting current condition is reached when the current becomes nearly constant. The slope of the current–

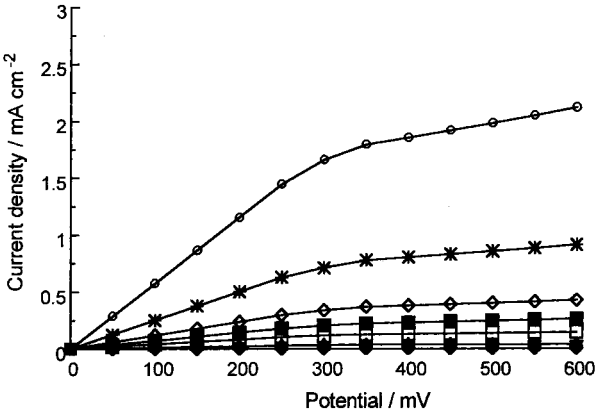

Fig. 3. Local current density polarization curves for $\bar{C}_b = 0.02$ M and $\Omega = 200$ rpm. (■) Total current density, r: (◆) 0.17; (✶) 0.33; (□) 0.5; (◇) 0.67; (✳) 0.79; (○) 0.92.

overpotential curve in Figure 3 does not become zero after the slope change, especially at the locations where the current density is relatively large, nevertheless the slope becomes much smaller, so we consider that the limiting current condition is reached around the time when a large slope change is observed. Based on our past work [4], the value of current density at 400 mV is taken to be the limiting current herein. It appears that the limiting current condition is reached almost simultaneously over the whole cathode surface, according to Figure 3. The limiting current density varies along the radius of the cathode: The current density is very low near the centre of the cathode, increases sharply in the radial direction, and becomes very high near the edge of the cell.

Figure 4(a) shows the local mass transfer rates, computed from the local limiting current values, for different Ekman numbers or rotating speeds. The mass transfer rate increases with decreasing *Ek*, as the solutal boundary layer becomes thinner. In all cases the limiting current is close to zero in the central area of the cathode and increases sharply towards the outer edge area. To explain this variation of mass transfer rate with radial position, it is necessary to describe the flow in the rotating cell. Referring to Figure 1, the flow is radially outward along the bottom wall (anode) with increasing radial velocity away from the centre. Along the top wall (cathode), where the local mass transfer rate is measured, the flow is inward from the outer edge with decreasing radial velocity toward the centre. As the velocity decreases in the flow direction along the cathode surface, the solutal boundary layer thickness increases sharply away from the edge so that the mass transfer occurs mainly in the edge region. There are two more reasons for the large mass transfer in the outer edge. In the outer edge region, the flow along the bottom wall turns towards the top wall (see Figure 1), and, as a result, the flow towards the top wall tends to keep the solutal boundary layer there thin. Another factor is that there exists a stratification of concentration of the cupric ions in the core region. Due to the centrifugal buoyancy, the concentration in the bulk solution is much higher near the edge than that near the centre. Consequently, the concentration difference between the top wall and the bulk solution becomes large near the edge. The fact that the mass transfer rate is increased appreciably in the outer edge region may be utilized in rotating Ni/Zn battery design to stabilize the active materials of the zinc electrode and prolong the recharging cycle-life. Figure 4(b) shows the local mass transfer rate along the radius, for different $Sc\,Ro_S$ numbers or bulk concentrations. The mass transfer rate increases with increasing $Sc\,Ro_S$, as the centrifugal buoyancy convection becomes stronger. The increasing mass transfer due to increasing bulk concentration is similar to that due to increasing rotating rate of the cell.

However, at different locations along the electrode, the $Sc\,Ro_S$ number affects the local mass transfer rate differently. Figure 5 shows local Sherwood number against $Sc\,Ro_S$ number for different locations. Due to the concentration stratification and different thickness of solutal boundary layer along the surface of the cathode, the slope of the local Sherwood number with

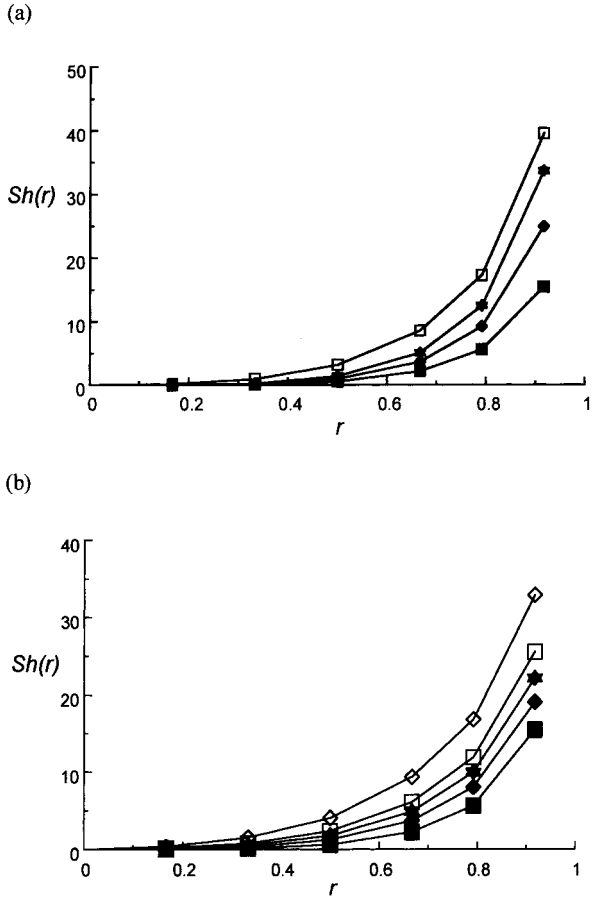

Fig. 4. Local mass transfer rates along the radius of electrode. (a) $Sc\,Ro_S = 5.3$, *Ek*: (■) 0.0028; (◆) 0.0014; (✶) 0.00092; (□) 0.00069, (b) $Ek = 0.0028$, $Sc\,Ro_S$: (■) 5.3; (◆) 10.7; (✶) 16; (□) 21.3; (◇) 42.7.

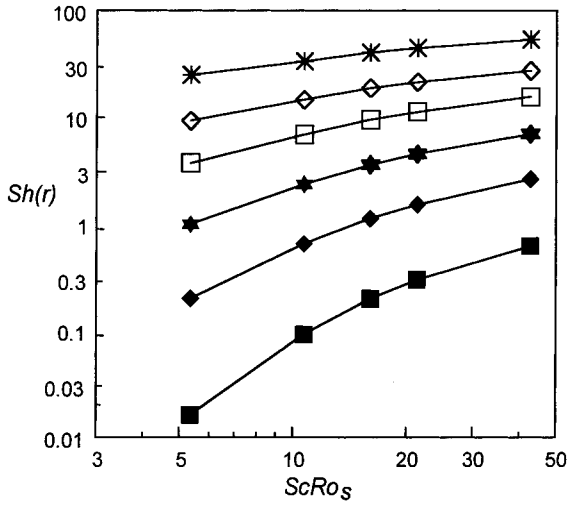

Fig. 5. Local Sherwood number against $Sc\,Ro_S$ number at different locations along the radius of cathode for $Ek = 0.003$. *r*: (■) 0.17; (◆) 0.33; (✶) 0.5; (□) 0.67; (◇) 0.79; (✳) 0.92.

respect to the $Sc\,Ro_S$ number also becomes a function of the location. In a double algorithmic chart, the slopes of the local mass transport rates with respect to $Sc\,Ro_S$ number are comparatively large for those near the centre and are small for those at the edge. The larger slope near the centre of the cathode implies that the local mass transfer rate is more sensitive to the $Sc\,Ro_S$ number (or bulk concentration) near the centre than at the edge area.

It is found in most of the present tests that the current is not exactly steady near the limiting current, unlike in our earlier tests with smaller test sections. This unsteady feature is described and discussed next. Two typical cases of local limiting current as a function of time are presented in Figure 6. In both cases the local current shows a certain degree of unsteadiness. In the case of 0.01 M bulk concentration and 100 rpm (Figure 6(a)), the relative amplitude of current fluctuation is less than 5%. The maximum fluctuation occurs near the outer edge due to strong centrifugal convection. The current fluctuation is much less over the rest of the cathode. For the conditions of 0.08 M bulk concentration and 200 rpm (Figure 6(b)), the relative amplitude of current fluctuation increases to 15%. Although the current fluctuation level is largest near the outer edge, the fluctuation is noticeable over most of the cathode. The fact that the limiting current density changes from steady to unsteady in a large diameter cell implies that there is a critical parameter that marks the onset of instability or turbulence in the rotating electrochemical cell.

In the present electrochemical system, the $Sc\,Ro_S$ number is larger than unity, so that the total mass transfer is dominated by the centrifugal convection. In this situation, the ratio of convection to diffusion is represented by the centrifugal Rayleigh number, Ra_R. We [4] have shown that the dimensionless total mass transfer rate, namely the total Sherwood number, scales with $Ra_R^{1/4}$. It is noted that the $\frac{1}{4}$-power law is based on laminar flow assumption. With dominant centrifugal convection, the present situation is similar to natural convection in vertical enclosures, at least globally, with the present Ra_R equivalent to the conventional Ra in natural convection. Also, the present global mass transfer problem is similar to natural convection heat transfer.

In Figure 7, the amplitudes of current fluctuation at the outer edge of the test cell are plotted as a function of centrifugal Rayleigh number. The amplitude of current fluctuation is about 5% of the mean current value at $Ra_R = 2 \times 10^{11}$. The value increases with increasing Ra_R. When Ra_R is near 10^{13}, the amplitude becomes about 15%. The result implies that a transition from laminar to turbulent convection takes place below Ra_R of around 10^{13}.

In Figure 8 the total Sherwood (or Nusselt) number is plotted as a function of centrifugal Rayleigh number. Our past mass transfer data and available heat transfer data are shown also for comparison. Hudson et al. [8] published heat transfer data in the range of centrifugal Rayleigh number between 10^7 and 10^9. Our earlier mass transfer work [4] covered the range 3×10^{10}–10^{12}. The data by Hudson et al. and a part of our earlier data show that $\overline{Sh}_R$ or $\overline{Nu}_R$ scales with $Ra_R^{1/4}$, as predicted by our scaling analysis. According to Figure 8, the $\frac{1}{4}$-power law is valid up to about Ra_R of 5×10^{11}. However, the

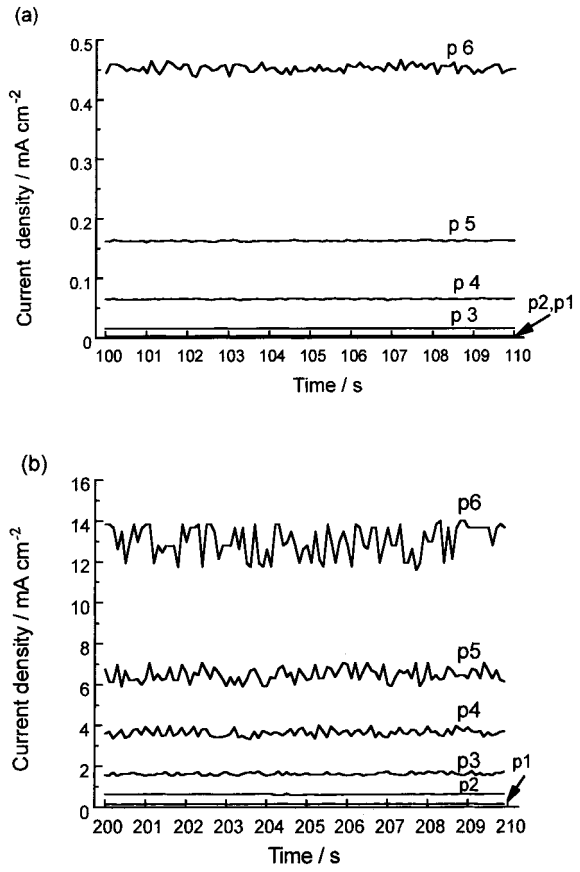

Fig. 6. Local limiting current against time. (a) $\bar{C}_b = 0.01$ M, $\Omega =$ 100 rpm, (b) $\bar{C}_b = 0.08$ M, $\Omega = 200$ rpm.

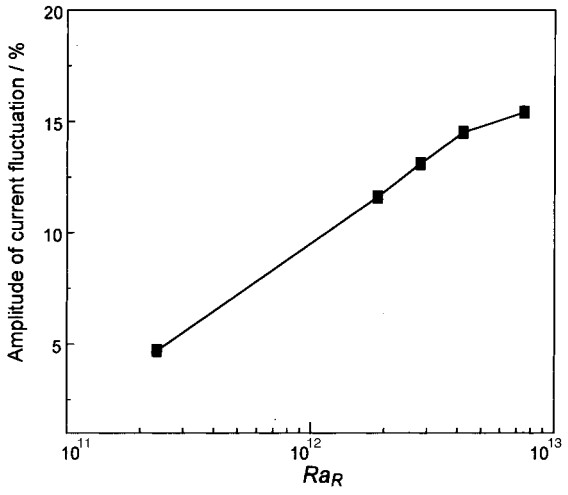

Fig. 7. Amplitude of current fluctuation vs. centrifugal Rayleigh number.

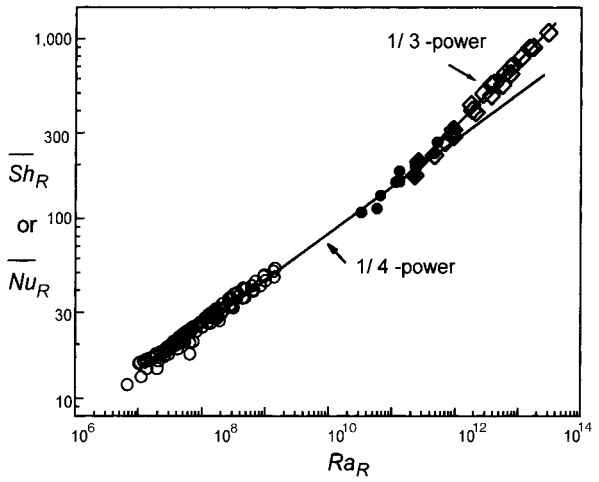

Fig. 8. Total Sherwood (or Nusselt) number vs. centrifugal Rayleigh number. (◇) Present data; (●) Weng et al. [4]; (○) Hudson et al. [8].

present data do not follow the 1/4-power law: the present mass transfer data are correlated well by $\overline{Sh}_R = 0.034\,Ra_R^{0.34}$. It is known that for natural convection along solid surfaces and for natural convection in enclosures the Nusselt scales generally with $Ra^{1/4}$ in the laminar range and with $Ra^{1/3}$ in the turbulent range for fluids with Pr larger than about unity. From the above data correlation it seems that a laminar-to-turbulent transition takes place when Ra_R is between 5×10^{11} and 10^{12}. That is the reason for the current fluctuations shown earlier.

Although the present problem is similar globally to natural convection in a vertical enclosure, the flow details are not the same. In natural convection the flow along the hot wall and that along the cold wall are symmetric (if changes of properties with temperature are negligible). In the present problem, the centrifugal acceleration increases with radius, which results in the aforementioned nonsymmetry of the flows along the cathode and anode. The flow velocity is high near the outer edge and the flow decelerates quickly in the flow direction along the cathode. It seems then that the flow near the outer edge is responsible for the transition in the present problem. More work is needed to clarify this point.

5. Conclusion

Mass transfer in a rotating shallow electrochemical cell was investigated in transient and turbulent flow regimes. By measuring the local limiting current densities at the cathode, the local mass transfer rates were determined. The centrifugal buoyancy enhances the mass transfer near the outer edge of the cathode and dominates the overall mass transfer rate. The centrifugal Rayleigh number is used to correlate the mass transfer data. When Ra_R is larger than about 10^{12}, the total Sherwood number is found to scale with $Ra_R^{1/3}$, instead of $Ra_R^{1/4}$ as in the laminar range. In the same range of Ra_R, the measured local current density fluctuates with time, the fluctuation level increasing with increasing Ra_R. It is concluded that the flow undergoes a laminar-to-turbulent transition. Since the local structures of the flow in the present configuration are different from those of better known natural convection in vertical enclosures, the flow transition mechanism is expected to be different in both cases.

Acknowledgements

We gratefully acknowledge the financial support by NASA Office of Life and Microgravity Science and Applications under grant NAG3-886.

References

1. F.R. Mclarnon and E.J. Cairns, *J. Electrochem. Soc.* **138** (1991) 645.
2. P. Tamminen, US Patent 4 684 585 (1987).
3. F.-B. Weng, 'Mass Transfer Process in Rotating Shallow Electrochemical Cells', PhD thesis, Case Western Reserve University, OHio (1997).
4. F.-B. Weng, Y. Kamotani and S. Ostrach, *Int. J. Heat Mass Transf.* **41** (1998) 2725.
5. Z. Cheng, 'Local Mass Transfer in Rotating Shallow Electrochemical Cells', MS thesis, Case Western Reserve University, OHio (1998).
6. J.R. Selman and C.W. Tobias, *Adv. Chem. Eng.* **10** (1978) 211.
7. C.R. Wilke, M. Eisenberg and C.W. Tobias, *J. Electrochem. Soc.* **100** (1958) 513.
8. J.L. Hudson, D. Tang and S. Abell, *J. Fluid Mech.* **86** (1978) 147.